Journal of Applied Analysis and Computation
Volume 6, Number 2, May 2016, 254–270
Website:http://jaac-online.com/
DOI:10.11948/2016021

NUMERICAL STUDY OF MIXED CONVECTION FLOW OF A MICROPOLAR FLUID TOWARDS PERMEABLE VERTICAL PLATE WITH CONVECTIVE BOUNDARY CONDITION

Ch. RamReddy[1,†], T. Pradeepa[1] and D. Srinivasacharya[1]

Abstract In this article, the mixed convective flow of a micropolar fluid along a permeable vertical plate under the convective boundary condition is analyzed. The scaling group of transformations is applied to get the similarity representation of the system of partial differential equations of the problem and then the resulting equations are solved by using Spectral Quasi-Linearisation Method. This study reveals that the dual solutions exists for certain values of mixed convection parameter. The outcomes are analyzed with dual solutions in detail. Effects of micropolar parameter, Biot number and suction/injection parameters on different flow profiles are discussed and depicted graphically.

Keywords Mixed convection, micropolar fluid, convective boundary condition, spectral Quasi-linearization method, dual solutions.

MSC(2010) 76A05, 76R99, 76M22, 76M60.

1. Introduction

In the past few decades, most of the researchers considered convective heat transfer problems either with wall temperature, heat flux or Newtonian heating in a Newtonian and/or non-Newtonian fluid. But, these models cannot explain the supply of heat with a finite heat capacity to the convecting fluid through a bounding surface. To overcome this, a novel mechanism for the heating process, known as *Convective Boundary Condition* (CBC), has drawn the involvement of many researchers. Besides, it is more realistic and general, especially in various technologies and industrial operations such as textile drying, transpiration cooling process, laser pulse heating, and so on. Aziz [2] showed that a similarity solution for the thermal boundary layer in a uniform stream of fluid under a convective boundary condition is possible if the convective heat transfer is proportional to $x^{-1/2}$, where x is the distance from the leading edge. In presence of the convective boundary condition, Makinde and Olanrewaju [13] illustrated that the combined effects of the Prandtl number and the Grashof number reduces the thermal boundary layer thickness along the plate, whereas Ishak [9] found that suction increases the surface shear stress and as a consequence increases the heat transfer rate at the surface. Subhashini etc [28, p11] discussed the simultaneous effects of thermal and concentration diffusions over a permeable surface in a Newtonian fluid, but RamReddy etc [22, p11] investigated the role of the thermal diffusion on combined convection in a nanofluid under the

[†]the corresponding author. Email address: chramreddy@nitw.ac.in; chittetiram@gmail.com (Ch. RamReddy)
[1]Department of Mathematics, National Institute of Technology Warangal-506004, India

convective boundary conditions. Recently, Ramesh and Gireesha [21] explored the effect of convective boundary conditions on the boundary layer flow of Maxwell fluid.

A great deal of involvement has been brought forth to illustrate the nonlinear relationship between the rate of strain and stress in non-Newtonian fluid models. But there is no single fluid flow model which undoubtedly exhibits all the properties of real fluids. Therefore, during the last century, several fluid models to characterize the real fluid behavior were proposed. Among these, micropolar fluids introduced by Eringen [7] have distinct features, such as microscopic effects arising from the local structure and micromotion of fluid elements, the presence of couple stresses, body couples and non-symmetric stress tensor. Micropolar fluids are the fluids with microstructure. Physically micropolar fluids may represent fluids consisting of rigid randomly oriented (or spherical) particles suspended in a viscous medium, where the deformation of fluid particles is ignored. More interesting aspects of the theory and application of micropolar fluids can be found in the books of Lukaszewicz [12] and Eremeyev etc [6, p11]. Mixed convection boundary layer flow of an incompressible micropolar fluid from an isothermal vertical flat plate has been considered by Jena and Mathur [10]. For an exhaustive discussion of the mixed convection in the boundary layers along a vertical surface in a micropolar fluid in the presence of double stratification and cross diffusion effects, the reader is referred to the works of Srinivasacharya and RamReddy ([26, 27]) (also see the references cited therein). Recently, Prakash and Muthtamilselvan [20] analyzed the radiation effect on fully developed flow of micropolar fluid between the two infinite parallel porous vertical plates in the presence of transverse magnetic field under convective boundary condition. Merely from the literature, it is noticed that most of the researchers found the local similarity and/or non-similarity solutions only.

In the recent past, several researchers are focused on obtaining the similarity solutions of the convective transport phenomena problems arising in fluid dynamics, aerodynamics, plasma physics, meteorology and some branches of engineering by using different procedures. One such procedure is *Lie group analysis*. The concept of Lie group analysis also called symmetry analysis initiated by *Sophus Lie* to determine transformations which map a given differential equation to itself and it combines almost all known exact integration techniques (For Ref. See [4, 19, 24, 25]). To provide a sophisticated, potent and systematic tool for generating the invariant solutions of the system of nonlinear partial differential equations with appropriate initial or boundary conditions, the scaling group transformations have been suggested by various researchers to study convective transport of different flow phenomena [see Hassanien and Hamad [8]; Seddeek etc [23, p11]; Kandasamy etc [11, p11] etc. are worth observing].

No effort has been gained so far to examine the similarity solution of mixed convection in a micropolar fluid on a permeable vertical plate under the convective boundary condition. Hence, the present investigation is aimed to find new similarity transformations, corresponding similarity solutions and to investigate mixed convection flow of a micropolar fluid on a permeable vertical plate under the convective boundary condition using the Lie group transformations. Besides, the influence parameters, namely, micropolar, suction/injection and convective heat transfer parameters on the physical quantities of the flow, heat and mass transfer coefficients are investigated. Further, the outcomes are analyzed with dual solutions in detail.

2. Mathematical Formulation

Consider the steady, laminar, mixed convective flow along a permeable vertical surface in an incompressible micropolar fluid. Choose the coordinate system such that the $\overline{x}$-axis is along the vertical plate and $\overline{y}$-axis normal to the plate. The physical model and coordinate system are shown in Fig.(1). The velocity of the outer flow is of the form $\overline{u}_e$, the free stream temperature and concentration are T_∞ and C_∞ respectively. The suction/injection velocity distribution is assumed to be v_w. The plate is either heated or cooled from left by convection from a fluid of temperature T_f with $T_f > T_\infty$ corresponding to a heated surface (assisting flow) and $T_f < T_\infty$ corresponding to a cooled surface (opposing flow) respectively. On the wall the solutal concentration is taken to be constant and is given by C_w.

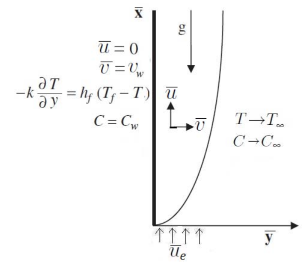

Figure 1. Physical model and coordinate system.

By employing Boussinesq approximation and making use of the standard boundary layer approximations, the governing equations for the micropolar fluid ([1,10]) are given by

$$\frac{\partial \overline{u}}{\partial \overline{x}} + \frac{\partial \overline{v}}{\partial \overline{y}} = 0, \tag{2.1}$$

$$\rho(\overline{u}\frac{\partial \overline{u}}{\partial \overline{x}} + \overline{v}\frac{\partial \overline{u}}{\partial \overline{y}}) = (\mu+\kappa)\frac{\partial^2 \overline{u}}{\partial \overline{y}^2} + \rho \overline{u}_e \frac{d\overline{u}_e}{d\overline{x}} + \kappa \frac{\partial \overline{\omega}}{\partial \overline{y}} + \rho g^* \left(\beta_T(\overline{x})(T-T_\infty) + \beta_C(\overline{x})(C-C_\infty)\right), \tag{2.2}$$

$$\rho j \left(\overline{u}\frac{\partial \overline{\omega}}{\partial \overline{x}} + \overline{v}\frac{\partial \overline{\omega}}{\partial \overline{y}}\right) = \gamma \frac{\partial^2 \overline{\omega}}{\partial \overline{y}^2} - \kappa\left(2\overline{\omega} + \frac{\partial \overline{u}}{\partial \overline{y}}\right), \tag{2.3}$$

$$\overline{u}\frac{\partial T}{\partial \overline{x}} + \overline{v}\frac{\partial T}{\partial \overline{y}} = \alpha \frac{\partial^2 T}{\partial \overline{y}^2}, \tag{2.4}$$

$$\overline{u}\frac{\partial C}{\partial \overline{x}} + \overline{v}\frac{\partial C}{\partial \overline{y}} = D \frac{\partial^2 C}{\partial \overline{y}^2}, \tag{2.5}$$

where $\overline{u}$ and $\overline{v}$ are the velocity components in $\overline{x}$ and $\overline{y}$ directions respectively, T is the temperature, C is the concentration, $\overline{\omega}$ is the component of microrotation whose direction of rotation lies in the $\overline{x}\,\overline{y}$-plane, g^* is the acceleration due to gravity, ρ is the density, μ is the dynamic coefficient of viscosity, $\beta_T(\overline{x})$ is the coefficient of thermal expansion, $\beta_C(\overline{x})$ is the coefficient of solutal expansions, κ is the vortex viscosity, j is the micro-inertia density, γ is the spin-gradient viscosity, α is the thermal diffusivity and D is the solutal diffusivity of the medium.

The boundary conditions are

$$\overline{u}=0,\ \ \overline{v}=v_w,\ \ \overline{\omega}=-n\frac{\partial \overline{u}}{\partial \overline{y}},\ \ -k\frac{\partial T}{\partial \overline{y}}=h_f(T_f-T),\ \ C=C_w \quad \text{at} \quad \overline{y}=0, \tag{2.6a}$$

$$\overline{u}=\overline{u}_e,\ \ \overline{\omega}=0,\ \ T=T_\infty,\ \ C=C_\infty \quad \text{as} \quad \overline{y}\to\infty, \tag{2.6b}$$

where, the subscripts w and ∞ indicate the conditions at the wall and at the outer edge of the boundary layer respectively, h_f is the convective heat transfer coefficient, k is the thermal conductivity of the fluid and n is a material constant. Further, the assumption $\gamma=\left(\mu+\frac{\kappa}{2}\right)j$ is incorporated to allow the field of equations predicts the correct behavior in the limiting case when the microstructure effects become negligible and the total spin $\overline{\omega}$ reduces to the angular velocity [1].

Introducing the following dimensionless variables

$$\left.\begin{aligned} &x=\frac{\overline{x}}{L},\ y=\frac{\overline{y}}{L}Re^{1/2},\ u=\frac{\overline{u}}{U_\infty},\ v=\frac{\overline{v}}{U_\infty}Re^{1/2},\\ &u_e=\frac{\overline{u}_e}{U_\infty},\ \omega=\frac{L^2}{\nu Re^{3/2}}\overline{\omega},\ \theta=\frac{T-T_\infty}{T_f-T_\infty},\ \phi=\frac{C-C_\infty}{C_w-C_\infty},\end{aligned}\right\} \tag{2.7}$$

where U_∞ is the reference velocity and $Re=\dfrac{U_\infty L}{\nu}$ is the global Reynold's number.

In view of the continuity equation (2.1), we introduce the stream function ψ by

$$u=\frac{\partial\psi}{\partial y},\quad v=-\frac{\partial\psi}{\partial x}. \tag{2.8}$$

Using (2.7) and (2.8) into (2.2)-(2.5), we get the following momentum, angular momentum, energy, and concentration equations

$$\begin{aligned}\Delta_1=&\frac{\partial\psi}{\partial y}\frac{\partial^2\psi}{\partial x\partial y}-\frac{\partial\psi}{\partial x}\frac{\partial^2\psi}{\partial y^2}-\left(\frac{1}{1-N}\right)\frac{\partial^3\psi}{\partial y^3}-\left(\frac{N}{1-N}\right)\frac{\partial\omega}{\partial y}-u_e\frac{du_e}{dx}\\ &-\frac{g^*\beta_T(\overline{x})(T_f-T_\infty)}{\nu^2Re^2}\theta-\frac{g^*\beta_C(\overline{x})(C_w-C_\infty)}{\nu^2Re^2}\phi=0,\end{aligned} \tag{2.9}$$

$$\Delta_2=\frac{\partial\psi}{\partial y}\frac{\partial\omega}{\partial x}-\frac{\partial\psi}{\partial x}\frac{\partial\omega}{\partial y}-\left(\frac{2-N}{2-2N}\right)\frac{\partial^2\omega}{\partial y^2}+\left(\frac{N}{1-N}\right)\left(2\omega+\frac{\partial^2\psi}{\partial y^2}\right)=0, \tag{2.10}$$

$$\Delta_3=\frac{\partial\psi}{\partial y}\frac{\partial\theta}{\partial x}-\frac{\partial\psi}{\partial x}\frac{\partial\theta}{\partial y}-\frac{1}{Pr}\frac{\partial^2\theta}{\partial y^2}=0, \tag{2.11}$$

$$\Delta_4=\frac{\partial\psi}{\partial y}\frac{\partial\phi}{\partial x}-\frac{\partial\psi}{\partial x}\frac{\partial\phi}{\partial y}-\frac{1}{Sc}\frac{\partial^2\phi}{\partial y^2}=0, \tag{2.12}$$

where ν is the kinematic viscosity, $N=\dfrac{\kappa}{\mu+\kappa}$ is the coupling number, $Pr=\dfrac{\nu}{\alpha}$ is the Prandtl number and $Sc=\dfrac{\nu}{D}$ is the Schmidt number.

Now the boundary conditions (2.6) become

$$\frac{\partial\psi}{\partial y}=0,\ \ \frac{\partial\psi}{\partial x}=f_w,\ \ \omega=-n\frac{\partial^2\psi}{\partial y^2},\ \ \frac{\partial\theta}{\partial y}=-Bi(1-\theta),\ \ \phi=1 \quad \text{at} \quad y=0, \tag{2.13a}$$

$$\frac{\partial\psi}{\partial y}=u_e,\ \ \omega=0,\ \ \theta=0,\ \ \phi=0 \quad \text{as} \quad y\to\infty, \tag{2.13b}$$

where $f_w = -\dfrac{Re^{1/2}}{U_\infty}\, v_w$ is the suction/injection parameter and $Bi = \dfrac{h_f\, L}{k\, Re^{1/2}}$ is the Biot number. It is worth mentioning that f_w determines the transpiration rate at the surface, with $f_w > 0$ for suction, $f_w < 0$ for injection, and $f_w = 0$ corresponds to an impermeable surface.

3. Similarity Solutions via Lie Group Analysis

A one-parameter scaling group of transformations which is a simplified form of Lie group transformation, is selected as ([11])

$$\left.\begin{aligned}&\Gamma : x^* = x\, e^{\varepsilon\, \alpha_1},\ y^* = y\, e^{\varepsilon\, \alpha_2},\ \psi^* = \psi\, e^{\varepsilon\, \alpha_3},\ \omega^* = \omega\, e^{\varepsilon\, \alpha_4},\ \theta^* = \theta\, e^{\varepsilon\, \alpha_5},\\ &\phi^* = \phi\, e^{\varepsilon\, \alpha_6},\ \beta_T^* = \beta_T\, e^{\varepsilon\, \alpha_7},\ \beta_C^* = \beta_C\, e^{\varepsilon\, \alpha_8},\ u_e^* = u_e\, e^{\varepsilon\, \alpha_9}.\end{aligned}\right\} \tag{3.1}$$

Here $\varepsilon \neq 0$ is the parameter of the group and $\alpha' s$ are arbitrary real numbers not all simultaneously zero. Equations (2.9)-(2.12) along with the boundary conditions (2.13) will remain invariant under the group of transformations in Eq.(3.1) if α_i's hold following relationship

$$\left.\begin{aligned}&\alpha_1 + 2\alpha_2 - 2\alpha_3 = 3\alpha_2 - \alpha_3 = \alpha_2 - \alpha_4 = -\alpha_5 - \alpha_7 = -\alpha_6 - \alpha_8 = \alpha_1 - 2\alpha_9,\\ &\alpha_1 + \alpha_2 - \alpha_3 - \alpha_4 = 2\alpha_2 - \alpha_4 = -\alpha_4 = 2\alpha_2 - \alpha_3,\\ &\alpha_1 + \alpha_2 - \alpha_3 - \alpha_5 = 2\alpha_2 - \alpha_5, \alpha_1 + \alpha_2 - \alpha_3 - \alpha_6 = 2\alpha_2 - \alpha_6,\\ &\alpha_1 - \alpha_3 = 0; -\alpha_4 = 2\alpha_2 - \alpha_3; \alpha_2 - \alpha_5 = 0 = -\alpha_5; \alpha_6 = 0; \alpha_2 - \alpha_3 = -\alpha_9.\end{aligned}\right\} \tag{3.2}$$

Using the procedure explained in the article by Uddin etc [29, p11] and Mutlag etc [17, p11], we have the following similarity transformations:

$$\left.\begin{aligned}&\eta = y, \quad \psi = x f(\eta), \quad \omega = x g(\eta),\\ &u_e = x, \quad \beta_T = \beta_{T_0} x, \quad \beta_C = \beta_{C_0} x, \quad \theta = \theta(\eta), \quad \phi = \phi(\eta),\end{aligned}\right\} \tag{3.3}$$

where β_{T_0} and β_{C_0} are constant thermal and mass coefficient of expansion.

Using Eq. (3.3) into Eq. (2.9)-(2.12), we get the following similarity equations

$$\left(\frac{1}{1-N}\right) f''' + f f'' + 1 - f'^2 + \left(\frac{N}{1-N}\right) g' + \lambda(\theta + \mathcal{B}\phi) = 0, \tag{3.4}$$

$$\left(\frac{2-N}{2-2N}\right) g'' + f g' - f' g - \left(\frac{N}{1-N}\right)(2g + f'') = 0, \tag{3.5}$$

$$\frac{1}{Pr}\theta'' + f\theta' = 0, \tag{3.6}$$

$$\frac{1}{Sc}\phi'' + f\phi' = 0, \tag{3.7}$$

where the primes indicate partial differentiation with respect to η alone. $Gr = \dfrac{g^* \beta_{T_0}(T_f - T_\infty)L^3}{\nu^2}$ is the thermal Grashof number, $Gc = \dfrac{g^* \beta_{C_0}(C_w - C_\infty)L^3}{\nu^2}$ is the solutal Grashof, $\mathcal{B} = \dfrac{Gc}{Gr}$ is the buoyancy ratio and $\lambda = \dfrac{Gr}{Re^2}$ is the mixed convection parameter. We also notice that $\lambda > 0$ and $\lambda < 0$ correspond to assisting flow and opposing flow respectively whereas $\lambda = 0$ produces forced convection flow problem. Boundary conditions (2.13) in terms of f, g, θ and ϕ become

$$\eta = 0: \ f(0) = f_w, \ f'(0) = 0, \ g(0) = -nf''(0), \ \theta'(0) = -Bi[1 - \theta(0)], \ \phi(0) = 1, \tag{3.8a}$$

$$\eta \to \infty: \ f'(\infty) = 1, \ g(\infty) = 0, \ \theta(\infty) = 0, \ \phi(\infty) = 0. \tag{3.8b}$$

4. Skin friction, Wall couple stress, Heat and Mass transfer coefficients

The wall shear stress and the wall couple stress are

$$\tau_w = \left[(\mu + \kappa)\frac{\partial \overline{u}}{\partial \overline{y}} + \kappa \overline{\omega}\right]_{\overline{y}=0} \quad \text{and} \quad m_w = \gamma \left[\frac{\partial \overline{\omega}}{\partial \overline{y}}\right]_{\overline{y}=0} \tag{4.1a}$$

and the heat and mass transfers from the plate respectively are given by

$$q_w = -k\left[\frac{\partial T}{\partial \overline{y}}\right]_{\overline{y}=0} \quad \text{and} \quad q_m = -D\left[\frac{\partial C}{\partial \overline{y}}\right]_{\overline{y}=0}. \tag{4.2a}$$

The non-dimensional skin friction $C_f = \dfrac{2\tau_w}{\rho \overline{u}_e^2}$, wall couple stress $M_w = \dfrac{m_w}{\rho \overline{u}_e^2 \overline{x}}$, the local Nusselt number $Nu_{\overline{x}} = \dfrac{q_w \overline{x}}{k(T_f - T_\infty)}$ and local Sherwood number $Sh_{\overline{x}} = \dfrac{q_m \overline{x}}{D(C_w - C_\infty)}$ are given by

$$\left.\begin{aligned} &C_f Re_{\overline{x}^{1/2}} = 2\left(\frac{1 - nN}{1 - N}\right) f''(0), \qquad M_w Re_{\overline{x}} = \left(\frac{2 - N}{2 - 2N}\right) g'(0) \\ &\frac{Nu_{\overline{x}}}{Re_{\overline{x}^{1/2}}} = -\theta'(0), \qquad \frac{Sh_{\overline{x}}}{Re_{\overline{x}^{1/2}}} = -\phi'(0), \end{aligned}\right\} \tag{4.3}$$

where $Re_{\overline{x}} = \dfrac{\overline{u}_e \overline{x}}{\nu}$ is the local Reynold's number.

5. Numerical Solution using the Spectral Quasilinearization Method(SQLM)

In this section, we introduce the quasilinearization method (QLM) for solving the governing system of Eqs.(3.4)-(3.7) along with the boundary conditions(3.8). This QLM is a generalization of the Newton-Raphson method and was proposed by Bellman and Kalaba [3] for solving nonlinear boundary value problems.

Assume that the solutions f_r, g_r, θ_r and ϕ_r of Eqs. (3.4)-(3.7) at the $(r+1)^{th}$ iteration are f_{r+1}, g_{r+1}, θ_{r+1} and ϕ_{r+1}. If the solutions at the previous iteration are sufficiently close to the solutions at the present iteration, the nonlinear components of the Eqs.(3.4)-(3.7) can be linearised using one term Taylors series for multiple variables so that the Eqs.(3.4)-(3.7) give the following iterative sequence of linear differential equations:

$$\left(\frac{1}{1-N}\right) f'''_{r+1} + a_{1,r}\, f''_{r+1} + a_{2,r}\, f'_{r+1} + a_{3,r}\, f_{r+1} + \left(\frac{N}{1-N}\right) g'_{r+1} + \lambda\,\theta_{r+1} + \lambda\,\mathcal{B}\,\phi_{r+1} = R_{1,r}, \tag{5.1}$$

$$\left(\frac{2-N}{2-2N}\right) g''_{r+1} + b_{3,r}\, g'_{r+1} + b_{4,r}\, g_{r+1} + b_{1,r}\, f'_{r+1} + b_{2,r}\, f_{r+1} - \left(\frac{N}{1-N}\right) f''_{r+1} = R_{2,r}, \tag{5.2}$$

$$c_{1,r}\, f_{r+1} + \frac{1}{Pr}\,\theta''_{r+1} + c_{2,r}\,\theta'_{r+1} = R_{3,r}, \tag{5.3}$$

$$d_{1,r}\, f_{r+1} + \frac{1}{Sc}\,\phi''_{r+1} + d_{2,r}\,\phi'_{r+1} = R_{4,r}, \tag{5.4}$$

where the coefficients $a_{s1,r}(s1 = 1,2,3)$, $b_{s2,r}(s2 = 1,2,..,4)$, $c_{s3,r}(s3 = 1,2)$, $d_{s4,r}(s4 = 1,2)$ and $R_{s5,r}(s5 = 1,2,..,4)$are known functions (from previous calculations) and are defined as

$$\begin{aligned}
&a_{1,r} = f_r,\ a_{2,r} = -2\, f'_r,\ a_{3,r} = f''_r,\ R_{1,r} = f_r\, f''_r - 1 - (f'_r)^2,\\
&b_{1,r} = -g_r,\ b_{2,r} = g'_r,\ b_{3,r} = f_r,\ b_{4,r} = -f'_r - \left(\frac{2N}{1-N}\right),\ R_{2,r} = f_r\, g'_r - f'_r\, g_r,\\
&c_{1,r} = \theta'_r,\ c_{2,r} = f_r,\ R_{3,r} = f_r\,\theta'_r,\\
&d_{1,r} = \phi'_r,\ d_{2,r} = f_r,\ R_{4,r} = f_r\,\phi'_r.
\end{aligned}$$

The above system (5.1) to (5.4) constitute a linear system of coupled differential equations with variable coefficients and can be solved iteratively using any numerical method for r = 1, 2, 3, ... In this work, as will be discussed below, the Chebyshev pseudo-spectral method was used to solve the QLM scheme (5.1) to (5.4) [For more details, one can refer the works of Motsa etc [15, p11] and [16, p11]].

The initial guesses to start the SQLM scheme for the system of equations (5.1)-(5.4) are chosen as functions that satisfy the boundary conditions as follows:

$$f_0(\eta) = f_w + \eta - 1 + e^{-\eta},\ g_0(\eta) = -n\, e^{-\eta},\ \theta_0 = \frac{Bi}{1+Bi}\, e^{-\eta},\ \phi_0 = e^{-\eta},$$

starting from these set of initial approximations f_0, g_0, θ_0, ϕ_0, the iteration schemes (5.1) to (5.4) can be solved iteratively for $f_{r+1}(\eta)$, $g_{r+1}(\eta)$, $\theta_{r+1}(\eta)$, $\phi_{r+1}(\eta)$ when r = 0, 1, 2,.... For this, we discretise the equation using the Chebyshev spectral collocation method. The basic idea behind the spectral collocation method is that the first appearance of a differentiation matrix D which is applied to approximate the differential coefficients of the unknown variables. In this procedure, the function $f(\eta)$ can be written as the matrix vector product

$$\frac{df}{d\eta} = \sum_{k=0}^{\overline{N}} D_{lk} f(\tau_k) = DF,\ \ l = 0,1,...,\overline{N}, \tag{5.5}$$

at the Gauss-Lobatto collocation points

$$\tau_j = \cos\frac{\pi j}{\overline{N}}, \qquad j = 0,1,2,...,\overline{N}, \tag{5.6}$$

where $\overline{N}+1$ is the number of collocation points (grid points), $D = \dfrac{2\mathcal{D}}{\eta_\infty}$ is the differentiation matrix and its entries are clearly defined in Canuto etc [5, p11], and $F = [f(\tau_0), f(\tau_1), ..., f(\tau_{\overline{N}})]^T$ is the vector function at the collocation points. Similar vector functions corresponding to g, θ and ϕ are denoted by G, θ and $\boldsymbol{\phi}$ respectively. Higher order derivatives are obtained as powers of D, that is

$$f^{(p)} = D^p F,\ g^{(p)} = D^p G,\ \theta^{(p)} = D^p \theta,\ \phi^{(p)} = D^p \phi, \tag{5.7}$$

where p is the order of the derivatives, η_∞ is a finite length that is chosen to be numerically large enough to approximate the conditions at infinity in the governing problem and τ is a variable used to map the truncated interval $[0, \eta_\infty]$ to the interval $[-1, 1]$ on which the spectral method can be implemented.

Substituting Eqs.(5.5)-(5.7) into Eqs. (5.1)-(5.4) leads to the matrix equation

$$\begin{bmatrix} A_{11} & A_{12} & A_{13} & A_{14} \\ A_{21} & A_{22} & A_{23} & A_{24} \\ A_{31} & A_{32} & A_{33} & A_{34} \\ A_{41} & A_{42} & A_{43} & A_{44} \end{bmatrix} \begin{bmatrix} F_{r+1} \\ G_{r+1} \\ \theta_{r+1} \\ \phi_{r+1} \end{bmatrix} = \begin{bmatrix} R_1 \\ R_2 \\ R_3 \\ R_4 \end{bmatrix}$$

where

$$A_{11} = \left(\frac{1}{1-N}\right) \mathrm{D}^3 + \mathrm{diag}[a_{1,r}]\, \mathrm{D}^2 + \mathrm{diag}[a_{2,r}]\mathrm{D} + \mathrm{diag}[a_{3,r}],\ A_{12} = \left(\frac{N}{1-N}\right) \mathrm{D},$$
$$A_{13} = \lambda \mathrm{I},\ A_{14} = \lambda \mathcal{B}\, \mathrm{I},$$
$$A_{21} = -\left(\frac{N}{1-N}\right) \mathrm{D}^2 + \mathrm{diag}[b_{1,r}]\, \mathrm{D} + \mathrm{diag}[b_{2,r}],$$
$$A_{22} = \left(\frac{2-N}{2-2N}\right) \mathrm{D}^2 + \mathrm{diag}[b_{3,r}]\, \mathrm{D} + \mathrm{diag}[b_{4,r}],\, A_{23} = 0,\ A_{24} = 0,$$
$$A_{31} = \mathrm{diag}[c_{1,r}],\quad A_{32} = 0,\quad A_{33} = \frac{1}{Pr} \mathrm{D}^2 + \mathrm{diag}[c_{2,r}]\, \mathrm{D},\quad A_{34} = 0,$$
$$A_{41} = \mathrm{diag}[d_{1,r}],\quad A_{42} = 0,\quad A_{43} = 0,\quad A_{44} = \frac{1}{Sc} \mathrm{D}^2 + \mathrm{diag}[d_{2,r}]\, \mathrm{D},$$
$$R_1 = R_{1,r},\quad R_2 = R_{2,r},\quad R_3 = R_{3,r},\quad R_4 = R_{4,r},$$

subject to reduced boundary conditions

$$f_{r+1}(0) = f_w,\ f'_{r+1} = 0,\ f'_{r+1}(\infty) = 1, \tag{5.8}$$
$$g_{r+1} = -n\, f''_{r+1}(0),\ g_{r+1}(\infty) = 0, \tag{5.9}$$
$$\theta'_{r+1}(0) = -Bi(1-\theta(0)),\ \theta_{r+1}(\infty) = 0, \tag{5.10}$$
$$\phi_{r+1}(0) = 1,\ \phi_{r+1}(\infty) = 0, \tag{5.11}$$

where I is an identity matrix, the size of the matrix 0 is $(\overline{N}+1)\times 1$ and diag[ ] is a diagonal matrix, all of size $(\overline{N}+1)\times(\overline{N}+1)$. f, g, θ and ϕ are the values of the functions f, g, θ and ϕ when evaluated at the grid points. The subscript r denotes the iteration number.

Table 1. Comparison of $f''(0)$ and $-\theta'(0)$ for mixed convection along a vertical flat plate in Newtonian fluids ([14]; [18, p11]) when $N=0$, $n=0$, $Pr=1$, $Bi\to\infty$ and $f_w=0$.

λ	$f''(0)$			$-\theta'(0)$		
	Merkin [14]	Nazar etc [18, p11]	Present	Merkin [14]	Nazar etc [18, p11]	Present
-1.0	0.6489	0.6497	0.648861	0.5067	0.5071	0.506658
-0.6	0.8963	0.8971	0.896272	0.5357	0.5360	0.535659
-0.2	1.1241	1.1250	1.124101	0.5597	0.5601	0.559725
0.0	1.2326	1.2336	1.232588	0.5705	0.5708	0.570462
0.6	1.5416	1.5428	1.541593	0.5990	0.5993	0.598949
1.0	1.7367	1.7380	1.736681	0.6156	0.6160	0.615581
3.0	2.6259	2.6282	2.625893	0.6817	0.6822	0.681721
5.0	3.4230	3.4264	3.422943	0.7315	0.7320	0.731504

6. Results and Discussions

It is noticed that the present problem reduces to forced convection heat and mass transfer along an impermeable vertical plate in a micropolar fluid without convective boundary condition when $f_w=0$, $Bi\to\infty$ and $\lambda=0$. Also, in the limit as $N\to 0$, the governing equations (2.2)-(2.5) reduce to the corresponding equations for a mixed convection heat and mass transfer in a viscous fluid. In order to validate the code generated, the results of the present problem have been compared with works of Merkin [14] and Nazar etc [18, p11] as a special case by taking $N=0$, $n=0$, $Pr=1$, $Bi\to\infty$ and $f_w=0$ and found that they are in good agreement, as shown in Tab. (1). In order to study the effects of coupling number N, suction/injection parameter f_w, Biot number Bi and material parameter n, computations were carried out in the cases of $\mathcal{B}=1.0$ and $Pr=0.71$, $Sc=0.22$.

Figs. 2(a)-5(d) represent the existence of dual solutions on dimensionless velocity, microrotation, temperature and concentration with effect of parameters namely coupling number, Biot number, suction/injection and material constant. In these figures, the solid line represents the first solution whereas the dash line represents the second solution. It can be observed that the dual solutions exist for ($\lambda\le\lambda_c$), where $\lambda_c=-1.42492$ is known as critical point, beyond this critical point the solution is unique.

The influence of the coupling number N on the dimensionless velocity, microrotation, temperature and concentration are illustrated in Figs. 2(a)-2(d) with existence of dual solutions for fixed values of other parameters. The coupling of linear and rotational motion arising from the micromotion of the fluid molecules is completely characterized by the coupling number N, where $N\to 0$ represents the non-polar fluid or viscous fluid. As N becomes large, the effect of microstructure becomes significant, whereas with a diminished value of N the individuality of the substructure is a lot less articulated. As N increases, it is found from Fig. 2(a) that the maximum velocity decreases in amplitude in both the cases of first and second solutions. It is significant to mention that the velocity of the micropolar fluid is less compared to that of viscous fluid case. It can be noted from Fig. 2(b) that the microrotation profiles tend to become flatter initially, then decreases with an increasing value of N. This happens because the vanishing of antisymmetric part of

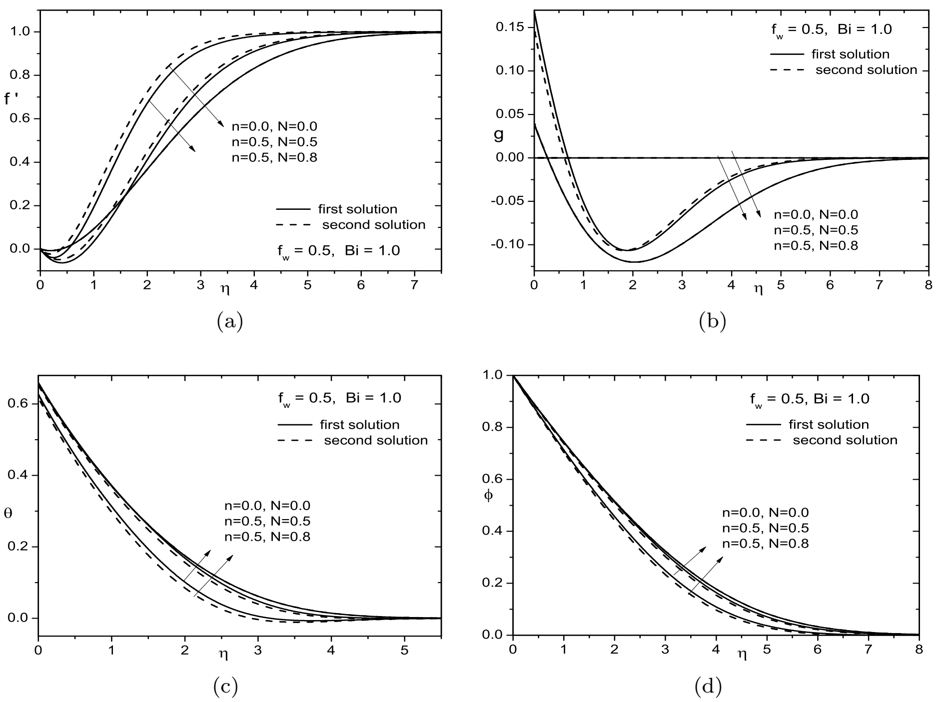

Figure 2. Effect of N on (a)Velocity, (b)Microrotation, (c)Temperature, and (d)Concentration profiles at $\lambda = -1.5$

the stress on the boundary corresponds to a weak concentration of microelements. Likewise, an increment in the value of N implies a higher vortex viscosity of fluid which promotes the microrotation of micropolar fluid. It is seen from Figs. 2(c) and 2(d) that the temperature and concentration of the fluid increases with the increase of coupling number N in both the cases of first and second solutions. The temperature and concentration of micropolar fluid are more than that of the viscous fluid case.

The Biot number Bi represents the ratio of the internal thermal resistance of a solid to the boundary layer thermal resistance. When $Bi = 0$ the plate is totally insulated, the internal thermal resistance of the plate is very high and no convective heat transfer to the cold fluid on the upper part of the plate takes place. Fig. 3(a) depicts the fluid velocity profiles with dual solutions for different values of Biot number. Generally, at the plate surface the fluid velocity is zero and rises gradually away from the plate to the free stream value satisfying the boundary conditions. It is interesting to observe that an increase in the strength of convective surface heat transfer Bi produces a substantial decrement in the fluid velocity within the momentum boundary layer. In both the cases of first and second solutions, Fig. 3(b) brings out the effect of Bi on the microrotation profile for fixed values of other parameters. As Bi increases, the microrotation showing reverse rotation near the two limits. Hence, the condition of vanishing of the antisymmetric part of the stress on the boundary results in a drastic change of the microrotation profiles. Given that convective heating increases with Biot number, $Bi \to \infty$ simulates the isothermal surface, which is clearly seen from the Fig. 3(c), where $\theta(0) = 1$ as $Bi \to \infty$. In fact, a high Biot number indicates higher internal thermal resistance of the plate than the boundary layer thermal resistance. The fluid temperature is maximum at the plate surface and decreases exponentially to zero value far out from the plate satisfying the boundary conditions. As a consequence, an increment in the Biot number leads to increase of fluid temperature efficiency. Fig. 3(d) illustrates the variation of dimensionless concentration for different values of Bi. An enhancement in concentration boundary layer thickness is seen with increasing values of Bi for both first and second solutions.

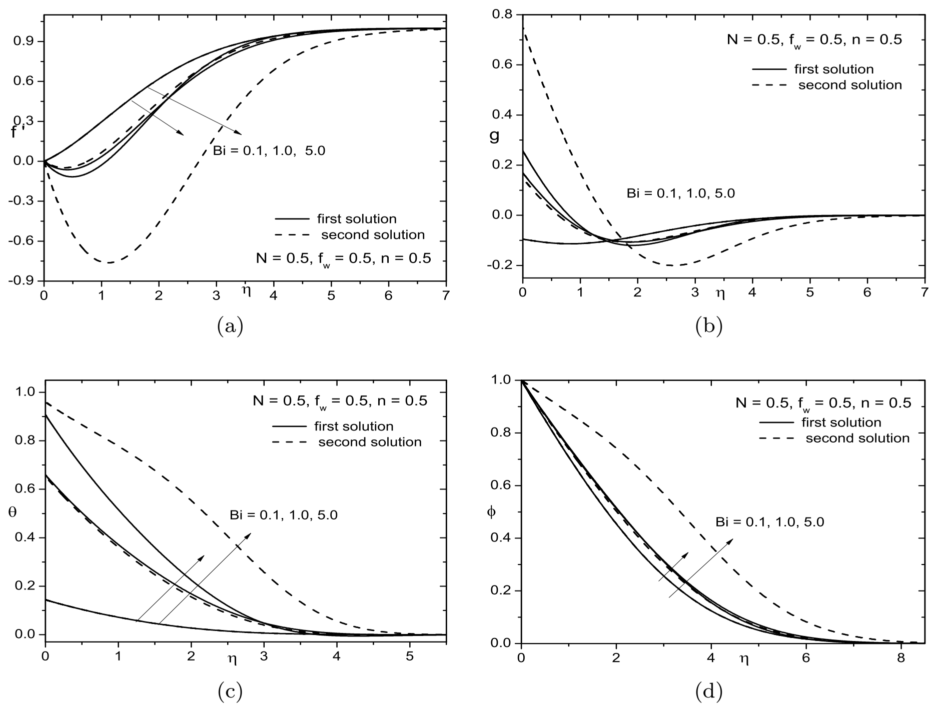

Figure 3. Effect of Bi on (a)Velocity, (b)Microrotation, (c)Temperature, and (d)Concentration profiles at $\lambda = -1.5$

The existence of dual solution for the effect of f_w on the velocity profile is shown in Fig. 4(a). Here, $f_w > 0$ represents the suction and $f_w < 0$ denotes the injection. The higher velocity is noticed in the case of suction when compared to the case of injection for both first and second solutions. From Fig. 4(b), it is seen that the microrotation profile within the boundary layer is showing reverse rotation near the two boundaries with the suction or injection parameter. For both the first and second solutions, the dimensionless temperature is depicted in Fig. 4(c) for different values of f_w. It is readable that the temperature of the micropolar fluid is less in the case of both injection and suction in comparison with the impermeable surface case ($f_w = 0$) for the first solution case, but reverse trend for second solution. Fig. 4(d) demonstrates the dimensionless concentration for different values of f_w. It is determined that the absorption of the fluid is more with impermeable surface case ($f_w = 0$), whereas less with suction and injection for the first and in case of second

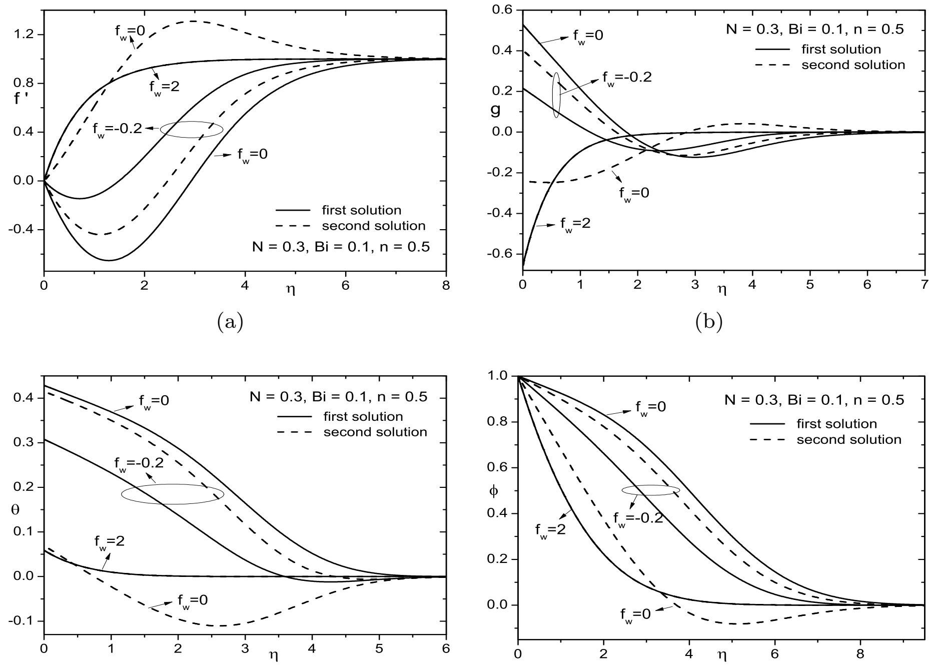

(a) (b) (c) (d)

Figure 4. Effect of f_w on (a)Velocity, (b)Microrotation, (c)Temperature, and (d)Concentration profiles at $\lambda = -1.5$

solution the injecton is more than suction in comparison with the impermeable surface case ($f_w = 0$).

In Figs. 5(a)-5(d), the effect of material parameter n on the dimensionless velocity, microrotation, temperature and concentration is presented by considering the dual solutions. Generally, when $n = 0$, equation (2.6a) yields $\overline{\omega}(x, 0) = 0$. This represents the case of concentrated particle flows in which the microelements close to the wall are not able to rotate. The case corresponding to $n = 1/2$ results in the vanishing of antisymmetric part of stress tensor and represents weak concentrations. The particle spin is equal to fluid vorticity at the boundary for the fine particle suspensions. From the Fig. 5(a), it reveals that as the value of n increases, the dimensionless velocity enhances in the cases of first and second solutions. From Fig. 5(b), for both first and second solution cases, we observe that the microrotation is increasing away from the plate within the boundary layer. It is clear from Figs. 5(c)-5(d) that with the increase of n, the thermal and solutal boundary layer thickness decrease in both the first and second solutions. Thus for $n = 0$, particles are not free to rotate near the surface, whereas, as n increases from 0 to 1/2, the microrotation term gets augmented and induces flow enhancement.

The effect of coupling number on skin friction, wall couple stress coefficients and heat and mass transfer rates against mixed convection parameter are presented in Figs. 6(a)-6(b). Fig. 6(a) depicts that the skin friction coefficient increases, but, except at $N = 0$ the wall couple stress decreases with an increasing coupling number. This is because of loss of micropolarity. From Fig. 6(b), it illustrates that

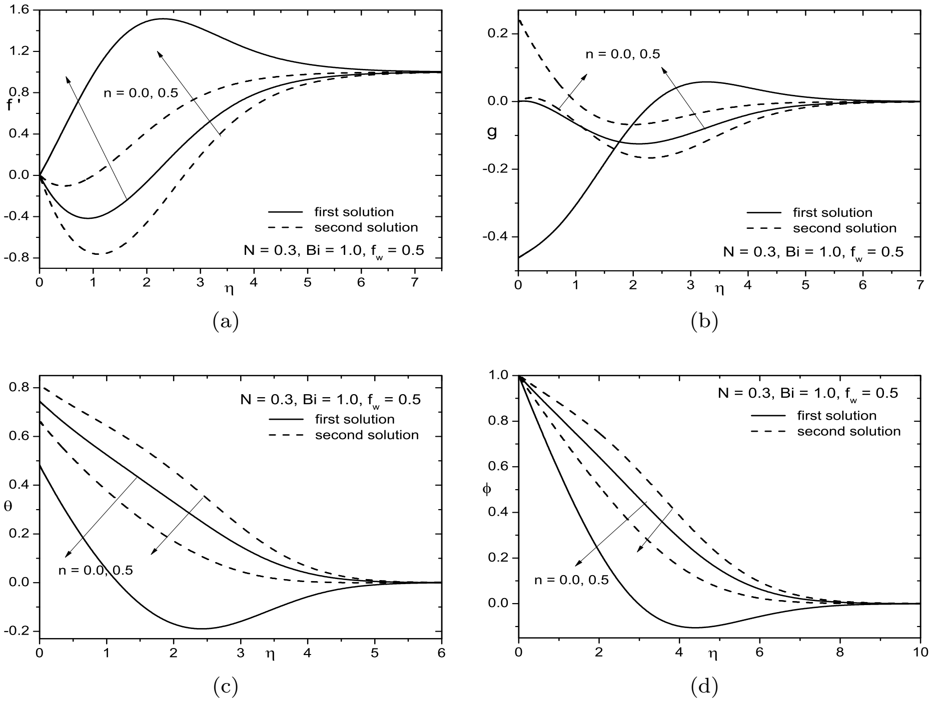

Figure 5. Effect of n on (a)Velocity, (b)Microrotation, (c)Temperature, and (d)Concentration profiles at $\lambda = -1.5$

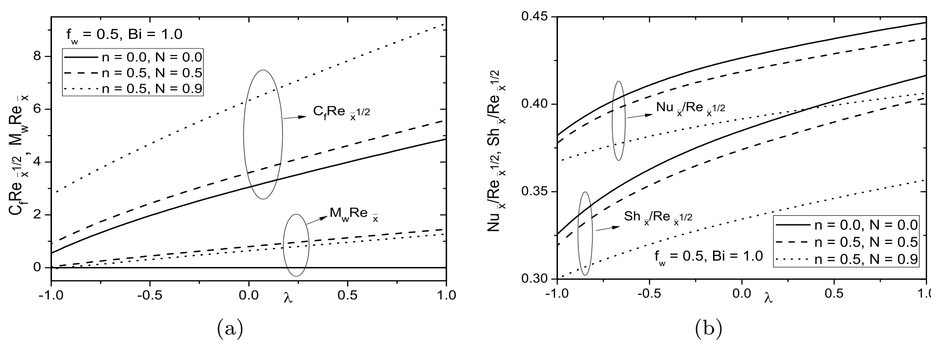

Figure 6. Effect of N on (a)skin friction and wall couple stress coefficients (b)Heat and mass transfer rates

with an increase of coupling number the heat and mass transfer rates decrease in the micropolar fluid comparing to the Newtonian fluid, they may be favorable in flow, temperature and concentration control of polymer processing. We also notice that the skin friction and wall couple stress coefficients, and heat and mass transfer rates increase with an increasing of mixed convection parameter λ.

Figs. 7(a)-7(b) show the influence of the Biot number on skin friction and wall couple stress coefficients, and heat and mass transfer rates against mixed convection parameter. These results display that with an increase of the Biot number both the

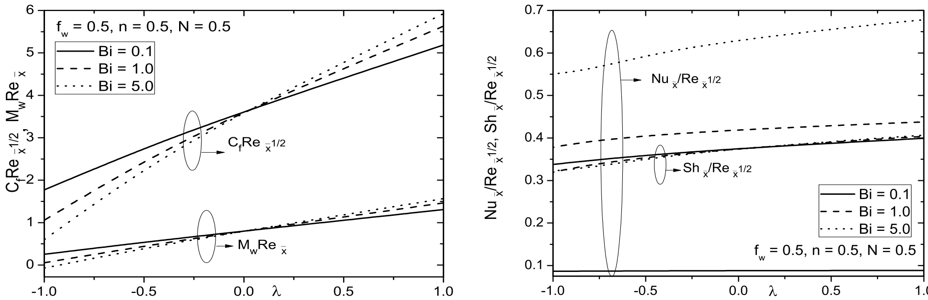

(a) (b)

Figure 7. Effect of Bi on (a)skin friction and wall couple stress coefficients (b)Heat and mass transfer rates

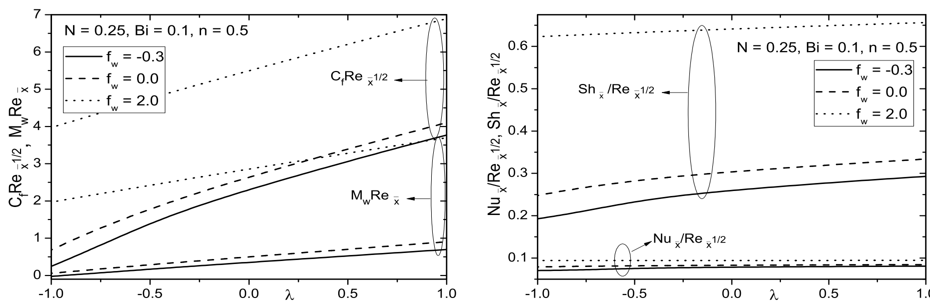

(a) (b)

Figure 8. Effect of f_w on (a)skin friction and wall couple stress coefficients (b)Heat and mass transfer rates

skin friction and wall couple stress coefficients are showing an opposite trend near the boundaries. Similarly the mass transfer rate also depicts the same behavior with that of skin friction and wall couple stress coefficients as shown in Fig. 7(b). Further, it is observed that the heat transfer rate enhances with the rising of Biot number.

The effect of suction/injection parameter on skin friction and wall couple stress coefficients, and heat and mass transfer rates against mixed convection parameter is analyzed in Figs. 8(a)-8(b). It is noticed that the skin friction and wall couple stress coefficients, and heat and mass transfer rates are higher in case of suction and lower in the injection case when comparison with the impermeable surface case.

Figs. 9(a)-9(b) depict the variation of material parameter n on skin friction and wall couple stress coefficients, and heat and mass transfer rates against mixed convection parameter. From Fig. 9(a), it is observed that the skin friction coefficient decreases whereas wall couple stress coefficient increases with increasing of material parameter. The heat and mass transfer rates are more in the case of $n = 0.5$ compared with that of $n = 0$ as shown in Fig. 9(b).

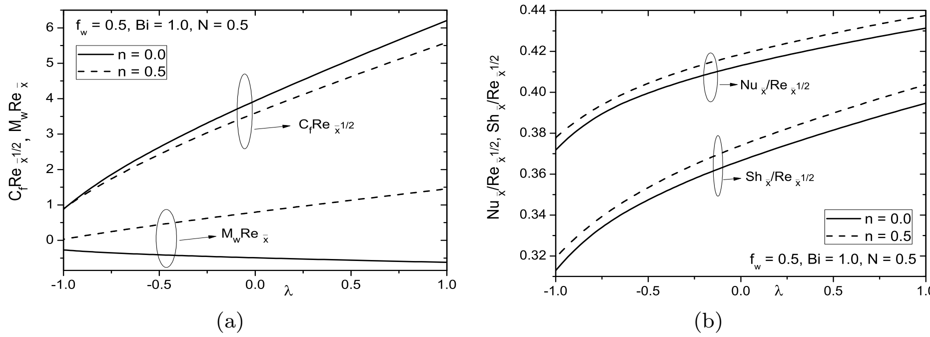

Figure 9. Effect of n on (a)skin friction and wall couple stress coefficients (b)Heat and mass transfer rates

7. Conclusions

In this paper, the similarity solution of the mixed convection flow along a permeable vertical plate of a micropolar fluid under the convective boundary condition is obtained. Utilizing a set of similarity variables, which are found using Lie group transformations, the governing equations are translated into a band of ordinary differential equations depending on several non-dimensional parameters. These equations are solved numerically using Spectral Quasi-Linearisation Method. This study reveals that the dual solutions exists for certain values of mixed convection parameter. The outcomes are analyzed with dual solutions in detail. The main findings are summarized as follows:

- The numerical results show that the velocity distribution, microrotation, the wall couple stress coefficient in the absence of polar fluid, heat and mass transfer rates are lower, but the skin friction coefficient, temperature and concentration distributions are higher with the increasing value of N.
- An increase in Biot number Bi, decreases in velocity distribution, whereas an increase in temperature and concentration distributions in the boundary layer for both first and second solutions. Further, with an increase in Biot number the skin friction, wall couple stress, mass transfer rate and microrotation are showing a reverse trend near the boundaries, but the heat transfer rate increases.
- It is noted that more velocity, skin friction and wall couple stress coefficients, heat and mass transfer rates, but less temperature and concentration distribution, in the case of suction compared to the case of injection. We remark that microrotation shows the opposite trend far away from the wall.
- It is found that more temperature, concentration distributions and skin friction, but less velocity distribution, wall couple stress, heat and mass transfer rates in the case of $n = 0$ compared to the case of $n = 1/2$.

Acknowledgements

The authors are thankful to the reviewers for their valuable suggestions and comments.

References

[1] G. Ahmadi, *Self-similar solution of incompressible micropolar boundary layer flow over a semi-infinite plate*, Int. J. Eng. Science, 14(1976), 639–646.

[2] A. Aziz, *A similarity solution for laminar thermal boundary layer over a flat plate with a convective surface boundary condition*, Commun Nonlinear Sci Numer Simulat, 14(2009), 1064–1068.

[3] R.E. Bellman and R.E. Kalaba, *Quasilinearisation and Non-linear Boundary-value Problems*, Elsevier, New York, 1965.

[4] G.W. Bluman and S.C. Anco, *Symmetry and Integration Methods for Differential Equations*, Springer-Verlag 2009.

[5] C. Canuto, M.Y. Hussaini, A. Quarteroni and T.A. Zang, *Spectral Methods Fundamentals in Single Domains*, Springer, Verlag, 2006.

[6] V.A. Eremeyev, L.P. Lebedev and H. Altenbach, *Foundations of Micropolar Mechanics*, Springer, Heidelberg, New York, 2013.

[7] A.C. Eringen, *Theory of Micropolar Fluids*, J. Math. and Mech., 16(1966), 1–18.

[8] I.A. Hassanien and M.A.A. Hamad, *Group theoretic method for unsteady free convection flow of a micropolar fluid along a vertical plate in a thermally stratified medium*, Applied Mathematical Modelling, 32(2008), 1099–1114.

[9] A. Ishak, *Similarity solutions for flow and heat transfer over a permeable surface with convective boundary condition*, Applied Mathematics and Computation, 217(2010), 837–842.

[10] S. Jena and M. Mathur, *Mixed convection flow of a micropolar fluid from an isothermal vertical plate*, Camp. Maths. with Appls., 10(1984), 291–304.

[11] R. Kandasamy, K. Gunasekaran and S.B.H. Hasan, *Scaling group transformation on fluid flow with variable stream conditions*, International Journal of Non-Linear Mechanics, 46(2011), 976–985.

[12] G. Lukaszewicz, *Micropolar fluids - Theory and Applications*, Birkhauser, Basel, 1999.

[13] O.D. Makinde and P.O. Olanrewaju, *Buoyancy effects on thermal boundary layer over a vertical plate with a convective surface boundary condition*, Journal of Fluids Engineering, 132(2010), 044502-1–4.

[14] J.H. Merkin, *Mixed convection from a horizontal circular cylinder*, International Journal of Heat and Mass Transfer 20(1977), 73–77.

[15] S.S. Motsa, P.G. Dlamini and M. Khumalo, *Spectral relaxation method and spectral quasilinearization method for solving unsteady boundary layer flow problems*, Advances in Mathematical Physics, 2014(2014). DOI:10.1155/2014/341964.

[16] S.S. Motsa, P. Sibanda, J.M. Ngnotchouye and G.T. Marewo, *A spectral relaxation approach for unsteady boundary-layer flow and heat transfer of a nanofluid over a permeable stretching/shrinking sheet*, Advances in Mathematical Physics, 2014(2014). DOI: 10.1155/2014/564942.

[17] A.A. Mutlag, M.J. Uddin, M.A.A. Hamad and A.I.M. Ismail, *Heat transfer analysis for falkner-skan boundary layer flow past a stationary wedge with slips boundary conditions considering temperature-dependent thermal conductivity*, Sains Malaysiana, 42(2013), 855–862.

[18] R. Nazar, N. Amin and I. Pop, *Mixed convection boundary-layer flow from a horizontal circular cylinder in micropolar fluids: case of constant wall temperature*, International Journal of Numerical Methods for Heat and Fluid Flow, 13(1)(2003), 86–109.

[19] M. Pakdemirli and M. Yurusoy, *Similarity transformations for partial differential equations*, SIAM Review, 40(1998), 96–101.

[20] D. Prakash and M. Muthtamilselvan, *Effect of radiation on transient MHD flow of micropolar fluid between porous vertical channel with boundary conditions of the third kind*, Ain Shams Engineering Journal, 5(2014), 1277–1286.

[21] G.K. Ramesh and B.J. Gireesha, *Influence of heat source/sink on a Maxwell fluid over a stretching surface with convective boundary condition in the presence of nanoparticles*, Ain Shams Engineering Journal, 5(2014), 991–998.

[22] Ch. RamReddy, P.V.S.N. Murthy, J.A. Chamkha and A.M. Rashad, *Soret effect on mixed convection flow in a nanofluid under convective boundary condition*, International Journal of Heat and Mass Transfer, 64(2013), 384–392.

[23] M.A. Seddeek, M.Y. Akl and A.M. Al-Hanaya, *Thermal radiation effects on mixed convection and mass transfer flow on vertical porous plate with heat generation and chemical reaction by using scaling group*, Journal of Natural Sciences and Mathematics 4(2010), 41–60.

[24] T. R. Sekhar and V.D. Sharma, *Similarity solutions for three dimensional Euler equations using Lie group analysis*, Applied Mathematics and Computation, 196(2008), 147–157.

[25] T. R. Sekhar and V.D. Sharma, *Similarity analysis of modified shallow water equations and evolution of weak waves*, Commun Nonlinear Sci Numer Simulat, 17(2012), 630–636.

[26] D. Srinivasacharya and Ch. RamReddy, *Mixed convection heat and mass transfer in a micropolar fluid with soret and dufour effects*, Adv. Appl. Math. Mech., 3(4)(2011), 389–400.

[27] D. Srinivasacharya and Ch. RamReddy, *Mixed convection in a doubly stratified micropolar fluid saturated non-Darcy porous medium*, Canadian J. Chemical Engineering, 90(2012), 1311–1322.

[28] S.V. Subhashini, N. Samuel and I. Pop, *Double-diffusive convection from a permeable vertical surface under convective boundary condition*, Int. Commun. Heat and Mass Transfer, 38(2011), 1183–1188.

[29] M.J. Uddin, W.A. Khan and A.I.M. Ismail, *MHD free convective boundary layer flow of a nanofluid past a flat vertical plate with Newtonian heating boundary condition*, Plos One 7(2012), e49499.